

JPMTR-2113  
DOI 10.14622/JPMTR-2113  
UDC 681.6-035.67|53.07

Original scientific paper | 153  
Received: 2021-09-09  
Accepted: 2021-12-03

# Modeling and analysis of the ink splitting factors influence on ink filling in offset printing

*Mykhailo Verkhola, Ulyana Panovyk, Myron Kalytka and Oleksandra Babych*

Department of Automation and Computer Technology,  
Ukrainian Academy of Printing,  
Pid Holoskom St. 19, 79020 Lviv, Ukraine

m.i.werh@gmail.com  
ulianapanovuk@gmail.com  
kalytka\_m@ukr.net

## Abstract

Currently, offset printing technology is used to manufacture a wide range of printing products. Given the trends to reduced print circulation, the issue of increasing the competitiveness of printing equipment by reducing the cost of ink and paper in printing press setup remains relevant, which is most effectively achieved by improving the accuracy of its pre-adjustment. The technical condition of printing equipment, the properties of ink and paper, climatic conditions in the production room, and other factors affect the distribution of ink flows in the inking and printing system (IPS). Obviously, the change in the ink splitting factors, which occurs under the influence of these aspects, will affect the accuracy of the pre-adjustment. The purpose of this study is to model and research the effect of ink splitting factors in the contact zones of rollers and cylinders on the process of its distribution and transmission in the IPS and its ink filling and to obtain information about the weight of ink splitting factors on the accuracy of the previous adjustment. To solve this problem, computer technology has been developed using the methods of automatic control theory, methods of mathematical modeling, theory of discrete systems, and MATLAB-Simulink interactive environment. A mathematical model of offset IPS was developed to implement the research technology, which describes the operation modes of all its components. The IPS simulator of the offset machine is constructed, which reproduces the technology of printing process. Simulation modeling and analysis of the ink splitting factors that influence the process of ink distribution and transmission in the IPS are carried out. The need to determine the reliable value of the ink splitting factors in the contact zones of the rollers and cylinders is substantiated. Computer technology makes it possible to determine the ink amount accumulating in the IPS during printing process and the ink thickness and volume on the surfaces of the imprints.

**Keywords:** mathematical model, signal graph, inking and printing system simulator, ink flow distribution, ink volumes

## 1. Introduction

Offset printing is the most common way of making printed products. According to the Joseph Webb, Frank Romano, and Smithers Pira released studies cited in Romano (2015), the share of offset printing was expected to be nowadays at 30–40 % among all methods of the total print volume. To further increase the competitiveness of offset printing, specialists need to improve the methods of its application and automatic adjusting systems.

The behavior of the ink flow in the contact zones of the rollers and cylinders and the mechanism of its division is largely related to the ink properties. Today there is a wide range of printing inks, different in their prop-

erties and purpose. Scientific publications (Kapović, et al., 2019; Ma, 2010; Shen, et al., 2017) claim that the ink splitting, in addition to its properties, is influenced by the plate coverage with printing elements, paper properties, the technical condition of printing equipment, climatic conditions in the production room, and other factors. But there is no information about the impact of these indicators on the ink distribution and splitting in the zone of two moving surfaces.

A significant contribution to the development of the theoretical and methodological foundations of inking unit modeling was made by Rech (1971). He proposed a computer method for estimating the ink transfer, which allows determining the ink thickness on individual areas of the rollers and cylinders surfaces. A model

of ink transfer between two cylindrical surfaces was proposed in the scientific work published by Chu, Lin, and Cai (2019). The research results of the temperature regime in the contact zone of two rotating rollers are presented. It is established that the ink temperature at the exit from the contact zone is higher than at the entrance. The maximum temperature appears in the transition zone between the exit from the contact zone and the non-extrusion zone. However, no information is provided on the effect of temperature change on the value of ink splitting. In Liu, Li, and Lu (2016), a model of ink transfer in an offset inking and printing system (IPS) was developed based on the Reynolds equation. As a result of modeling, a directly proportional dependence of an ink layer thickness in the contact zone of the rollers on their equivalent radius is established. However, there is no information on the parameters of the ink microflows splitting at the contact zones of the IPS elements.

The difficulty of solving this problem is due to the peculiarities of offset printing (MacPhee, 1998). Depending on the properties of the printing ink and the printing speed, the nature of the rupture of the ink layer changes, namely the formation of ink threads, which negatively affect the quality of printed products (Vlachopoulos, Claypole and Bould, 2010; Claypole, Williams and Deganelo, 2012). The analysis of published works allows stating the fact of the absence of a uniform approach to the mathematical description of inking devices, transfer, and splitting of ink. The mathematical description of the ink transfer process is realized using a system of algebraic equations that reflect the ink addition and division in the contact zones of the rollers and cylinders, assuming that the ink layer is split in half.

Analysis of publications shows that information about the specific value of the ink splitting factor in the process of its transportation from the ink supply device to the blanket cylinder (BC) in these works is missing. However, it should be noted that the scientific work included in Handbook of print media (Kipphan, 2001) presents the experimental results conducted on a specially designed model of the sequentially structured IPS. Based on these studies, it was found that without dampening solution the ink splitting factor at the contact zones of the rollers and cylinders close to the printing plate varies from 0.45 to 0.50 with a change in the frequency of axially oscillating distributor roller (OR). With dampening solution, the value of these factors can increase (Kipphan, 2001). But this experiment was performed with a constant ink supply, and there is no information on how the change in the magnitude of the ink splitting factor affects the ink redistribution in the IPS, and, accordingly, its thickness on the surface of the imprints.

## 2. Materials and methods

### 2.1 Object of research

It is extremely difficult and expensive to study the influence of ink splitting factors in the contact zones of rollers and cylinders on the amount of ink supplied by the ink feed system with the help of measuring equipment. It is proposed to solve this problem by modeling the process of ink distribution and transfer in IPS, and this requires the development of appropriate computer technology. We choose the Heidelberg GTO-52 offset inking and printing system as the object of research. In our study, the IPS is considered as a summation of ink supply device, inking unit, and printing unit, in which take place the processes of supply, distributing, circulating direct and reverse ink flows, forming and application of uniform, technologically necessary layer of ink on the surface of the printing form. The IPS scheme of the offset machine Heidelberg GTO-52 is given in Figure 1. An ink is discontinuously transmitted from the ink fountain roller (FR) to the OR 1 by the vibrator roller (VR). Next, the ink flows circulate on the surfaces of the rollers and cylinders, summing up when entering the places of their contacts and splitting at the outlet. On the printing elements of the form (plate), which is fixed on the plate cylinder (PC), the ink is transmitted by form rollers 6, 7, 11, 13. The IPS contains four ORs (1, 3, 5, and 12), which simultaneously with the rotational movement perform reciprocating axial movement. From the surface of the form, the ink is transferred to the BC, which in the area of contact with the impression cylinder (IC) applies the ink to the printed material (P).

### 2.2 Signal graph of the offset inking and printing system

According to the IPS scheme of the machine (Figure 1) we build a signal graph, which clearly shows the transmission of direct and reverse ink flows in the IPS during replication of printed products, a fragment of which for the first and last zone is shown in Figure 2. The vertices at the graph input correspond to the ink thicknesses of the zonal supply. The graph nodes reflect the volumes of ink flows at the contact points of the IPS elements. The nodes of the signal graph are connected by segments and arcs, which reflect the transmission operators of the ink flows between the contact zones of the rollers and cylinders. The segments at the graph output reflect the ink transfer operators in the appropriate zones of the imprint. Ink transfer operators reflect the value of ink splitting and the time of its transportation between adjacent contact points at the surfaces of rollers and cylinders:  $B_i$  – in the direction from the FR to the plate;  $H_i$  – in the opposite direction. Their mathematical description is presented in Equation [3] in section 2.3.

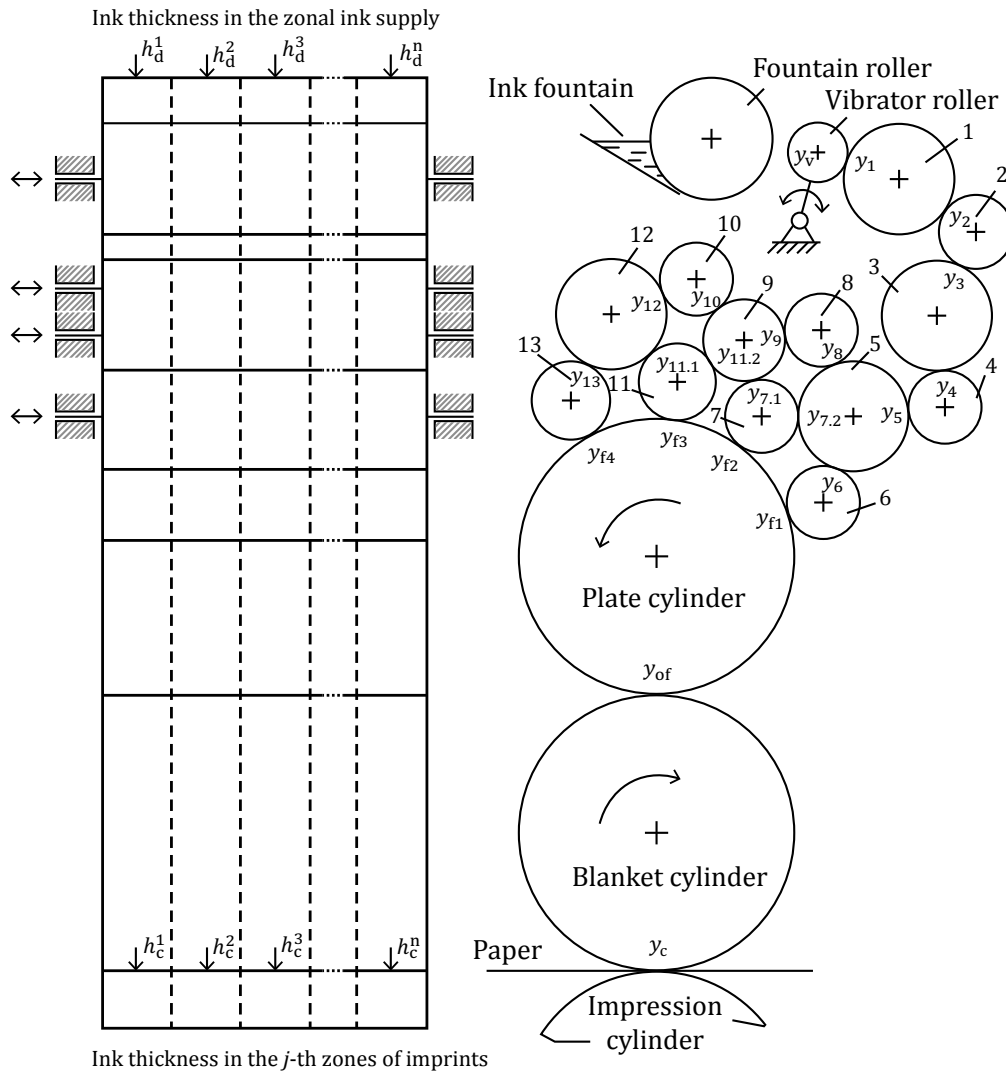


Figure 1: The inking and printing system scheme of the offset machine Heidelberg GTO-52

**2.3 Mathematical model of the inking and printing system**

When developing a mathematical model, we make the following assumptions: the diameters of the rollers and cylinders correspond to the diameters of the corresponding elements of the IPS of the GTO-52; the diameter of the PC is set taking into account the thickness of the printing form, and the diameter of the BC taking into account the thickness of the offset blanket; slipping in contact zones of rollers and cylinders is absent; pressure in the contact zones is neglected; linear velocities of the ink rollers and cylinders surfaces are the same; the surfaces of the IPS elements are (in axial direction) conventionally divided into zones, the number of which is equal to the number of inks supply regulators; the time of ink microflow passage on the surface of the IPS elements with a length of 1 mm corresponds to one relative unit; the period of OR move-

ment in the axial direction corresponds to two work cycles of the offset printing machine.

Further, for variables was accepted: cross-sections of ink flows in the contact zones and on the surfaces of the IPS elements, and cross-sections of ink flows at the inlet and transmission to the imprints (Figure 3).

Based on the accepted assumptions and results of works of Verkhola and Kalytka (2019) according to the signal graph scheme and Figure 3, a system of equations (Equation [1]) is compiled that describes ink distribution and its transfer from the ink fountain device to imprints in the *j*-th zone of the IPS.

Since the process of ink transfer in the IPS is discrete-continuous, it was used the mathematical apparatus of discrete Laplace transform, presented in the form of *z*-transform to describe it.



$$\begin{aligned}
s_d^j(z) &= b_z h_d^j(z); y_v^j(z) = s_d^j(z) + s_{rv}^j(z); s_{rd}^j(z) = H_d^j(z) y_v^j(z); \\
s_{pv}^j(z) &= [B_{1v}^j(z) H_v^j(z) + B_v^{*j}(z) B_{vd}^j(z)] y_v^j(z) + B_v^{*j}(z) P_d^j(z) H_v^{*j}(z) y_1^j(z); \\
y_1^j(z) &= s_{pv}^j(z) + s_{r1}^j(z) + s_{r1}^{j(j-1)}(z) + s_{r1}^{j(j+1)}(z); s_{p1}^j(z) = H_1^j(z) y_2^j(z); \\
s_{rv}^j(z) &= H_v^j(z) P_g^j(z) B_v^j(z) y_v^j(z) + [H_v^j(z) H_{v1}^j(z) + H_{dv}^j(z) H_v^{*j}(z)] y_1^j(z); \\
y_2^j(z) &= s_{p1}^j(z) + s_{p1}^{j(j-1)}(z) + s_{p1}^{j(j+1)}(z) + s_{r2}^j(z); s_{p2}^j(z) = B_2^j(z) y_2^j(z); \\
s_{r1}^j(z) &= H_1^j(z) y_2^j(z); s_{r1}^{j(j-1)}(z) = H_1^j(z) y_2^{j-1}(z); s_{r1}^{j(j+1)}(z) = H_1^j(z) y_2^{j+1}(z); \\
y_3^j(z) &= s_{p2}^j(z) + s_{r3}^j(z) + s_{r3}^{j(j-1)}(z) + s_{r3}^{j(j+1)}(z); s_{p3}^j(z) = B_3^j(z) y_3^j(z); \\
s_{p3}^{j(j-1)}(z) &= B_3^{j(j-1)}(z) y_3^{j-1}(z); s_{p3}^{j(j+1)}(z) = B_3^{j(j+1)}(z) y_3^j(z); s_{r2}^j(z) = H_2^j(z) y_3^j(z); \\
y_4^j(z) &= s_{p3}^j(z) + s_{p3}^{j(j-1)}(z) + s_{p3}^{j(j+1)}(z) + s_{r4}^j(z); s_{p4}^j(z) = B_4^j(z) y_4^j(z); \\
s_{r3}^j(z) &= H_3^j(z) y_4^j(z); s_{r3}^{j(j-1)}(z) = H_3^{j(j-1)}(z) y_4^{j-1}(z); s_{r3}^{j(j+1)}(z) = H_3^{j(j+1)}(z) y_4^{j+1}(z); \\
y_5^j(z) &= s_{p4}^j(z) + s_{r5.3}^j(z) + s_{r5.3}^{j(j-1)}(z) + s_{r5.3}^{j(j+1)}(z); s_{p5}^j(z) = B_5^j(z) y_5^j(z); \\
s_{p5}^{j(j-1)}(z) &= B_5^{j(j-1)}(z) y_5^{j-1}(z); s_{p5}^{j(j+1)}(z) = B_5^{j(j+1)}(z) y_5^{j+1}(z); s_{r4}^j(z) = H_4^j(z) y_5^j(z); \\
y_6^j(z) &= s_{r5.2}^j(z) + s_{r5.2}^{j(j-1)}(z) + s_{r5.2}^{j(j+1)}(z) + s_{r6}^j(z); s_{p6}^j(z) = B_6^j(z) y_6^j(z); \\
s_{r5.3}^j(z) &= H_{5.3}^j(z) y_6^j(z); s_{r5.3}^{j(j-1)}(z) = H_{5.3}^{j(j-1)}(z) y_6^{j-1}(z); s_{r5.3}^{j(j+1)}(z) = H_{5.3}^{j(j+1)}(z) y_6^{j+1}(z); \\
y_{7.1}^j(z) &= s_{r7}^j(z) + s_{r9.2}^j(z); s_{p7.1}^j(z) = B_{7.1}^j(z) y_{7.1}^j(z); s_{r9.3}^j(z) = H_{9.3}^j(z) y_{7.1}^j(z); \\
y_{7.2}^j(z) &= s_{p7.1}^j(z) + s_{r5.1}^j(z) + s_{r5.1}^{j(j-1)}(z) + s_{r5.1}^{j(j+1)}(z); s_{p7.2}^j(z) = B_{7.2}^j(z) y_{7.2}^j(z); \\
s_{r5.2}^j(z) &= H_{5.2}^j(z) y_{7.2}^j(z); s_{r5.2}^{j(j-1)}(z) = H_{5.2}^{j(j-1)}(z) y_{7.2}^{j-1}(z); s_{r5.2}^{j(j+1)}(z) = H_{5.2}^{j(j+1)}(z) y_{7.2}^{j+1}(z); \\
y_8^j(z) &= s_{p5}^j(z) + s_{p5}^{j(j-1)}(z) + s_{p5}^{j(j+1)}(z) + s_{r8}^j(z); s_{p8}^j(z) = B_8^j(z) y_8^j(z); \\
s_{r5.1}^j(z) &= H_{5.1}^j(z) y_8^j(z); s_{r5.1}^{j(j-1)}(z) = H_{5.1}^{j(j-1)}(z) y_8^{j-1}(z); s_{r5.1}^{j(j+1)}(z) = H_{5.1}^{j(j+1)}(z) y_8^{j+1}(z); \\
y_9^j(z) &= s_{p8}^j(z) + s_{r9.3}^j(z); s_{p9}^j(z) = B_9^j(z) y_9^j(z); s_{r8}^j(z) = H_8^j(z) y_9^j(z); \\
y_{10}^j(z) &= s_{p9}^j(z) + s_{r10}^j(z); s_{p10}^j(z) = B_{10}^j(z) y_{10}^j(z); s_{r9.1}^j(z) = H_{9.1}^j(z) y_{10}^j(z); \\
y_{11.1}^j(z) &= s_{r12.1}^j(z) + s_{r12.1}^{j(j-1)}(z) + s_{r12.1}^{j(j+1)}(z) + s_{r11}^j(z); s_{p11.1}^j(z) = B_{11.1}^j(z) y_{11.1}^j(z); \\
s_{r12.2}^j(z) &= H_{12.2}^j(z) y_{11.1}^j(z); s_{r12.2}^{j(j-1)}(z) = H_{12.2}^{j(j-1)}(z) y_{11.1}^{j-1}(z); s_{r12.2}^{j(j+1)}(z) = H_{12.2}^{j(j+1)}(z) y_{11.1}^{j+1}(z); \\
y_{11.2}^j(z) &= s_{p11.2}^j(z) + s_{r9.1}^j(z); s_{p11.2}^j(z) = B_{11.2}^j(z) y_{11.2}^j(z); s_{r9.2}^j(z) = H_{9.2}^j(z) y_{11.2}^j(z); \\
y_{12}^j(z) &= s_{p10}^j(z) + s_{r12.2}^j(z) + s_{r12.2}^{j(j-1)}(z) + s_{r12.2}^{j(j+1)}(z); s_{r10}^j(z) = H_{10}^j(z) y_{12}^j(z); \\
s_{p12}^j(z) &= B_{12}^j(z) y_{12}^j(z); s_{p12}^{j(j-1)}(z) = B_{12}^{j(j-1)}(z) y_{12}^{j-1}(z); s_{p12}^{j(j+1)}(z) = B_{12}^{j(j+1)}(z) y_{12}^j(z); \\
y_{13}^j(z) &= s_{p12}^j(z) + s_{p12}^{j(j-1)}(z) + s_{p12}^{j(j+1)}(z) + s_{r13}^j(z); s_{p13}^j(z) = B_{13}^j(z) y_{13}^j(z); \\
s_{r12.1}^j(z) &= H_{12.1}^j(z) y_{13}^j(z); s_{r12.1}^{j(j-1)}(z) = H_{12.1}^{j(j-1)}(z) y_{13}^{j-1}(z); s_{r12.1}^{j(j+1)}(z) = H_{12.1}^{j(j+1)}(z) y_{13}^{j+1}(z); \\
y_{f1}^j(z) &= s_{p6}^j(z) + s_{rf}^j(z); s_{pf1}^j(z) = B_{f1}^j(z) y_{f1}^j(z); s_{r6}^j(z) = H_6^j(z) y_{f1}^j(z); \\
y_{f2}^j(z) &= s_{p7.2}^j(z) + s_{pf1}^j(z); s_{pf2}^j(z) = B_{f2}^j(z) y_{f2}^j(z); s_{r7}^j(z) = H_7^j(z) y_{f2}^j(z); \\
y_{f3}^j(z) &= s_{p11.2}^j(z) + s_{pf2}^j(z); s_{pf3}^j(z) = B_{f3}^j(z) y_{f3}^j(z); s_{r11}^j(z) = H_{11}^j(z) y_{f3}^j(z); \\
y_{f4}^j(z) &= s_{p13}^j(z) + s_{pf3}^j(z); s_{pf4}^j(z) = B_{f4}^j(z) y_{f4}^j(z); s_{r13}^j(z) = H_{13}^j(z) y_{f4}^j(z); \\
y_{of}^j(z) &= s_{pf4}^j(z) + s_{rof}^j(z); s_{pof}^j(z) = B_{of}^j(z) y_{of}^j(z); s_{rf}^j(z) = H_f^j(z) y_{of}^j(z); \\
y_c^j(z) &= s_{pof}^j(z); s_c^j = B_c^j y_c^j(z); s_{rof}^j(z) = H_{of}^j(z) y_c^j(z)
\end{aligned}$$

where  $y_i^j(z)$  is a  $z$ -image of the cross-sectional areas of the ink flows at the contact points of the rollers and cylinders;  $j$  are regulation zones of ink supply;  $y_{fi}^j(z)$  is a  $z$ -image of the cross-sectional areas of the ink flows at the contact points of the printing form fixed on the plate cylinder with the form rollers 6, 7, 11, 13;  $y_{of}^j(z), y_c^j(z)$  are  $z$ -images of ink cross-sections in the  $j$ -th contact zones of the BC with the form and paper;

$s_{pi}^j(z), s_{ri}^j(z)$  are  $z$ -images of the cross-sectional areas of direct and reverse ink flows, transmitted in the circular direction by the  $j$ -th zones of rollers' and cylinders' surfaces;  $s_d^j(z)$  is a  $z$ -image of the cross-sectional areas of the ink flows supplied to the input of IPS;  $h_d^j(z)$  is the thickness of the zonal ink supply;  $s_{rd}^j(z)$  is  $z$ -image of the cross-sectional area of the ink flows returned to the ink fountain;  $s_{pv}^j(z), s_{rv}^j(z)$  are  $z$ -images of cross-

sectional areas of forward and reverse ink flows in the  $j$ -th zones of the VR surface;  $s_{\text{pfi}}^j(z)$ ,  $s_{\text{rf}}^j(z)$  are  $z$ -images of the cross-sectional areas of the forward and reverse ink flows, modulated by the printing form that transmitted by the  $j$ -th zones of its surface;  $s_{\text{por}}^j(z)$ ,  $s_{\text{rof}}^j(z)$  are  $z$ -images of the cross-sectional areas of the forward and reverse ink flows transmitted by the  $j$ -th zones of the BC surface;  $s_c^j(z)$  is  $z$ -image of cross-sectional areas of ink flows transmitted to the  $j$ -th zones of imprints;  $h_c^j(z) = s_c^j(z)/b_z$  is ink thickness in the  $j$ -th zones of imprints ( $b_z$  is the width of the  $j$ -th ink supply zone);  $H_d^j(z)$  is transfer operator of ink return flows volumes' in the  $j$ -th zones of the FR;  $B_v(z)$ ,  $H_v(z)$ , and  $B_v^*(z)$ ,  $H_v^*(z)$  are transfer operators of direct and return ink flows volumes' by the VR during contact with the FR and the first OR;  $B_{\text{vd}}^j(z)$ ,  $B_{\text{1v}}^j(z)$  and  $H_{\text{v1}}^j(z)$ ,  $H_{\text{vd}}^j(z)$  are operators of ink transfer by VR from the FR to the first OR and in the opposite direction;  $B_i^{j(j-1)}(z)$ ,  $B_i^{j(j+1)}(z)$  and  $H_i^{j(j-1)}(z)$ ,  $H_i^{j(j+1)}(z)$  are transfer operators of direct and reverse ink flows volumes' during the movement of the OR to the right and left;  $B_{\text{f1}}^j(z)$ ,  $B_{\text{f2}}^j(z)$ ,  $B_{\text{f3}}^j(z)$ ,  $B_{\text{f4}}^j(z)$  are transfer operators of ink volumes' by printing form;  $B_{\text{of}}^j(z)$ ,  $H_{\text{of}}^j(z)$  are transfer operators of direct and reverse ink flows volumes' by the BC;  $B_c^j$  is transfer operator of the ink volumes in the  $j$ -th zone of the imprint's surface.

Based on the results of previous scientific work (Verkhola and Huk, 2009; Verkhola, et al., 2015), the operators of ink transfer by the ink fountain device in  $z$ -images can be represented as follows:

$$\begin{aligned} B_v^j(z) &= [P_g(z)\alpha_v + \bar{P}_g(z)]z^{-p_v}; \\ B_v^{*j}(z) &= P_d(z)z^{-p_v}; \\ H_d^j(z) &= P_g(z)(1 - \alpha_v)z^{-p_d}; \\ H_v^j(z) &= P_g(z)z^{-r_v}; \\ H_v^{*j}(z) &= P_g(z)y_1P_d(z)z^{-r_v}; \\ B_{\text{vd}}^j(z) &= z^{-r_v}P_g(z)z^{-p_{1d}}; \\ B_{\text{1v}}^j &= \bar{P}_g(z)z^{-p_{1d}}; \\ H_{\text{dv}}^j(z) &= \bar{P}_d(z)z^{-r_{d1}}; \\ H_{\text{v1}}^j(z) &= z^{-p_v}\bar{P}_d(z)z^{-r_{d1}} \end{aligned} \quad [2]$$

where  $P_g(z)$ ,  $P_d(z)$  are the operators that specify the duration of the joint movement of the VR with the FR and the OR 1, and their inversions  $\bar{P}_g(z)$ ,  $\bar{P}_d(z)$ ;  $\alpha_v$  is ink splitting factor at the contact point of the VR with the FR;  $z^{-b_d}$  is the duration of FR rotation to a certain angle during the total supply of the ink pulse of width  $b_d$ ;  $z^{-p_d}$ ,  $z^{-r_d}$  are transport delays of ink transfer from the fountain to the contact place with the VR and in the opposite direction;  $z^{-p_v}$ ,  $z^{-r_v}$  are transport delays of direct and return ink flows transmission by the surface of the VR in relative units;  $z^{-p_{1d}}$  is the time of the VR stand near the FR in the sum of the time of its movement to the OR in relative units;  $z^{-r_{d1}}$  is the time of VR movement from the first OR to the FR in the

sum with the standing time before the beginning of the FR rotation in relative units. When entering the relative time, the description of the process of ink distributes and transferring does not depend on the rotation speed of the rollers and cylinders.

Transfer operators of direct and reverse ink flows in the circular direction can be represented in Equation [3]:

$$\begin{aligned} B_i^j(z) &= \alpha_i z^{-p_i}; \\ H_i^j(z) &= (1 - \alpha_{i+1})z^{-r_i}; \\ B_{\text{fi}}^j(z) &= \alpha_{\text{fi}} F(z)z^{-p_{\text{fi}}}; \\ H_{\text{fi}}^j(z) &= (1 - \alpha_{\text{fi}})z^{-r_{\text{fi}}}; \\ B_{\text{of}}^j &= \alpha_{\text{of}} z^{-p_{\text{of}}}; \\ H_{\text{of}}^j(z) &= (1 - \beta)z^{-r_{\text{of}}}; \\ B_c^j(z) &= \beta \end{aligned} \quad [3]$$

where  $\alpha_i$ ,  $\alpha_{\text{fi}}$ ,  $\alpha_{\text{of}}$  are ink splitting factors in the contact zones of the rollers and cylinders;  $F(z)$  is the ink transfer operator at the  $j$ -th zone of the printing form;  $\beta$  is the ink transfer coefficient from the surface of the BC to the printed material;  $z^{-p_i}$ ,  $z^{-r_i}$ ,  $z^{-p_{\text{fi}}}$ ,  $z^{-p_{\text{of}}}$ ,  $z^{-r_{\text{of}}}$  are transport delays of ink transfer by IPS elements in the circular direction between their contact points.

Formation operators of the printing elements placement in the  $j$ -th zones of the printing form surface, based on the results of Verkhola, et al. (2019), can be represented as follows:

$$\begin{aligned} F^j(z) &= z^{-b_0} \left( 1 - z^{-\alpha_1^j} + z^{-(\alpha_1^j + b_1^j)} - z^{-(\alpha_1^j + b_1^j + \alpha_2^j)} \right. \\ &\quad \left. + z^{-(\alpha_1^j + b_1^j + \dots + b_{m-1}^j + \alpha_n^j)} \right) (1 - z^{-d_f})^{-1} \end{aligned} \quad [4]$$

where  $b_0$  is the displacement of the image beginning of the printing elements relative to the form;  $\alpha_i^j$ ,  $b_i^j$  are transport delays of ink movement at a distance corresponding to the sizes of printing and blank elements in the  $j$ -th zone of the form;  $d_f$  is the duration of one revolution of the plate cylinder in relative units.

## 2.4 Simulator of the inking and printing system

Based on the functional scheme (Figure 1), the signal graph (Figure 2), and the mathematical model presented in Equation [1], a simulator of the offset printing machine GTO-52 was developed in the MATLAB-Simulink environment (Tyagi, 2012; MathWorks, 2020), which is presented in Figure 4. During the construction of the simulator, we assume that the number of ink transfer zones by the surfaces of the IPS elements is equal to the number of zones in its supply regulation ( $n = 16$ ) in the offset printing machine GTO-52. The geometric dimensions of the rollers and cylinders, corresponding to the dimensions of IPS elements, are set due to transport delays in the ink

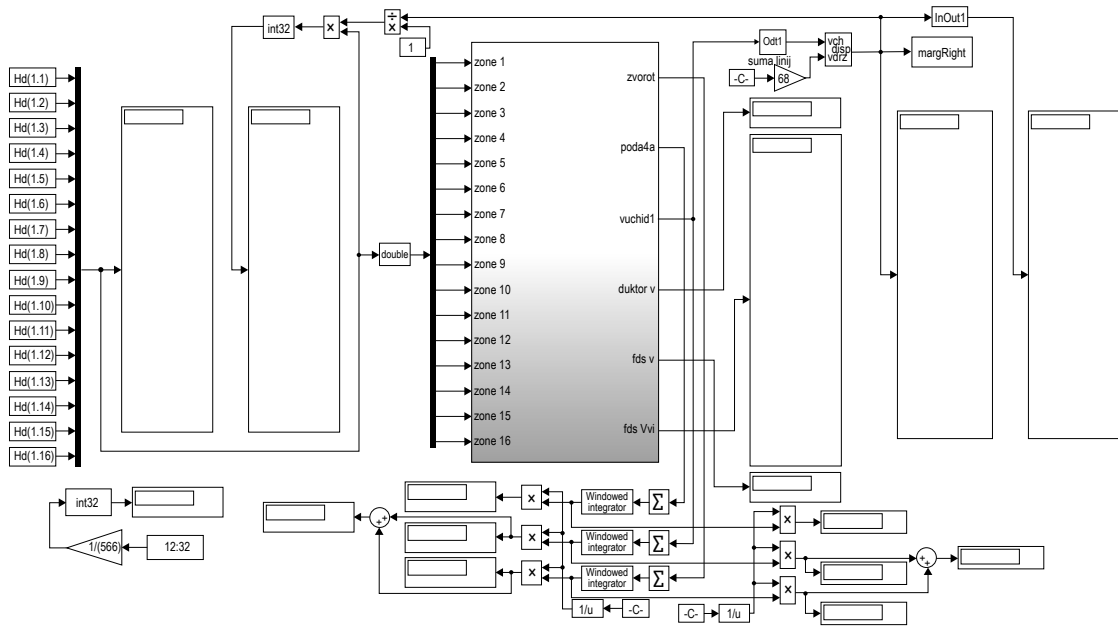


Figure 4: Scheme of the offset printing machine GTO-52 simulator

transfer operators. The ink transfer coefficient in the contact zones of the BC with the paper is taken equal to 0.7, the widths of the supply zones are the same and are  $b_z = 32$  mm. Using expression presented in Equation [4], a subsystem of the simulator was built, which generates the parameters of the printing form.

The constructed simulator is used to study the influence of ink splitting factors in the contact zones of rollers and cylinders on the distribution of ink flow volumes in the IPS. We set the thickness of the zonal ink supply  $h_a$  and the value of the total ink supply  $b_a$ . By changing the ink splitting factors, we conduct a series of experiments of the IPS model working for the printing form with different values of the coefficients corresponding to the form's area filing by printing elements  $k_z$ . The form's filing coefficient is defined as the ratio of the printing elements area to the printing form area. The adequacy of the ink transfer process reproduction is confirmed by the balance of ink supply and its selection when the system enters the steady mode. As a result of the simulation, we determine the ink volumes  $V_i$  that accumulate on the surfaces of IPS elements, as well as the ink thicknesses and its volumes on the surface of the imprints  $h_c$ . The ink volumes on the surface of each roller, cylinder, and imprint are determined using the appropriate blocks, which implement the following mathematical expression in Equation [5]:

$$\begin{aligned}
 V_i(z) &= \sum_{j=1}^{16} V_{p_i}^j + \sum_{r_i=1}^{16} V_{r_i}^j(z) \\
 &= \sum_{j=1}^{16} \left( \sum_{k=1}^{a_f} (z^{-1} + z^{-2} + z^{-3} + z^{-p_i}) S_{p_i}^j(z) \right. \\
 &\quad \left. + z^{-r_i} S_{p_i}^j(z) \right)
 \end{aligned}
 \tag{5}$$

where  $V_{p_i}^j, V_{r_i}^j(z)$  are the volumes of direct and reverse ink flows that accumulate in the  $j$ -th zones of the IPS elements surfaces.

Based on the information obtained, we analyze the nature of the ink distribution in the IPS and its ink filling.

### 3. Results and discussion

From the analysis of scientific publications, it can be concluded that the value of the ink splitting factors in the contact zones of the IPS elements is not a constant. Therefore, we assumed that splitting factor  $\alpha_i$  can be in the range from 0.40 to 0.50. Using the simulator for  $\alpha_i = 0.40, \alpha_i = 0.45$  and  $\alpha_i = 0.50$  we determined the parameters of the input task with the value of the total ink supply  $b_a = 30$  mm based on the condition that the ink thickness on the imprints surface is  $1 \mu\text{m}$ . We set the obtained values of the input task at different values of  $\alpha_i$  and performed simulations before the IPS enters the operating mode. The modeling process automatically determines the ink volumes  $V_i$  that accumulate on the elements of the IPS during printing and the ink volumes  $V_p$  and thicknesses  $h_c$  on the imprints surfaces. The obtained data are summarized in Table 1. As the ink splitting factors  $\alpha_i$  increase from 0.40 to 0.45, the ink volume  $V_{\text{IPS}}$  that accumulates in the IPS decreases by 2 times. And with the increase of  $\alpha_i$  to 0.50, the ink amount in the system decreases by 2.9 times.

In the next step, we expanded the values range of the ink splitting factors to 0.56 and set different values of the zonal ink supply thicknesses. At constant values

of the input task parameters, we conducted a series of model experiments by changing the ink splitting factors  $\alpha_i$  in the range from 0.40 to 0.56. The obtained results are summarized in Table A.1 and Table A.2 (Appendix A). According to Table A.1 we constructed a diagram of the ink thicknesses zonal distribution at the output of the IPS for different values of the factors, which is shown in Figure 5.

Table 1: Distribution of ink volumes  $V_i$  in the IPS at  $k_z = 1.0$ , for the listed parameters  $\alpha_i$ ,  $h_d$  and  $h_c$

	$\alpha_i = 0.40$	$\alpha_i = 0.45$	$\alpha_i = 0.50$
	$h_d = 156 \mu\text{m}$	$h_d = 74 \mu\text{m}$	$h_d = 53 \mu\text{m}$
Elements	$h_c = 0.998 \mu\text{m}$	$h_c = 0.992 \mu\text{m}$	$h_c = 1.006 \mu\text{m}$
IPS	$V_i (\times 10^3 \text{mm}^3)$	$V_i (\times 10^3 \text{mm}^3)$	$V_i (\times 10^3 \text{mm}^3)$
FR	17.300	8.025	5.644
VR	0.740	0.268	0.138
1	3.004	1.197	0.559
2	1.776	0.786	0.404
3	1.331	0.672	0.381
4	0.645	0.382	0.245
5	0.492	0.347	0.254
6	0.259	0.211	0.176
7	0.237	0.204	0.182
8	0.551	0.319	0.194
9	0.344	0.254	0.197
10	0.331	0.244	0.185
11	0.492	0.293	0.187
12	0.577	0.365	0.241
13	0.358	0.261	0.198
PC	0.546	0.470	0.426
BC	0.248	0.245	0.251
IPS	29.231	14.298	10.064
P	0.174	0.171	0.175

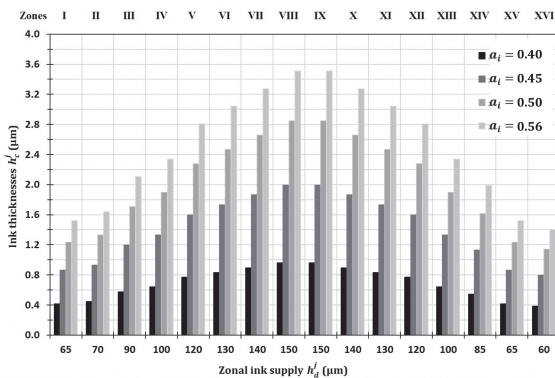


Figure 5: Ink thicknesses in the  $j$ -th zones I to XVI on the imprints with  $k_z = 1.0$ , at different ink splitting factors

As can be seen from the diagram, increasing the values of ink splitting factors in the contact zones of the rollers and cylinders significantly affects the ink thickness on the imprints. Thus, with an increase in  $\alpha_i$  from 0.40

to 0.45, the ink thickness in all zones of the imprints increases 2.1 times, and with an increase  $\alpha_i$  to 0.56 it increases 3.7 times. According to Table A.2, we constructed a diagram to analyze the distribution of ink flows volumes on the rollers' and cylinders' surfaces, as shown in Figure 6. When obtaining imprints at  $\alpha_i = 0.40$ , the ink accumulates mainly at the input of the IPS, and with increasing splitting factors it is redistributed to the output of the system with a simultaneous decrease of its amount on the rollers and cylinders surfaces. The influence of splitting factors on the ink amount accumulated at the input of the IPS is shown in the diagram in Figure 7. For the lowest  $\alpha_i$  the ink volume on the surface of roller 1 is  $2143 \text{mm}^3$ . As  $\alpha_i$  changes to 0.45, the ink volume decreases by 17 %, and as  $\alpha_i$  increases to 0.56, it decreases by 68 %, respectively.

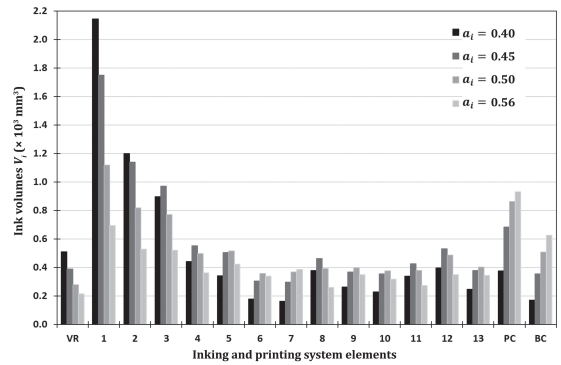


Figure 6: Distributions of ink flow volumes in the IPS at obtaining imprints with  $k_z = 1.0$ , when the values of  $\alpha_i$  are changed

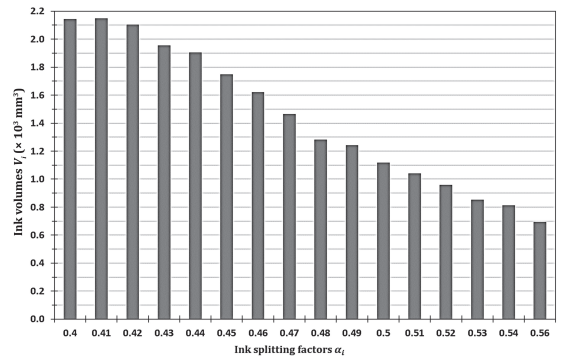


Figure 7: Dependence of the ink volume on the roller 1 surface on the factor  $\alpha_i$  when obtaining imprints with  $k_z = 1.0$

A completely different nature of the ink flow volumes distribution is observed in the case of change of  $\alpha_i$  on the surfaces of the form rollers (Figure 8) and the PC and BC (Figure 9).

As can be seen from Figure 8 different ink volumes accumulate on the surfaces of the form rollers when obtaining imprints with  $k_z = 1.0$  for  $\alpha_i = 0.40$ . Thus,

on the form roller 7, the ink volume is the smallest,  $V_7 = 163 \text{ mm}^3$ , and on roller 11 it is the largest,  $V_{11} = 338 \text{ mm}^3$ , and this ratio is 2.1.

The total ink volume on the four form rollers 6, 7, 11, 13 is  $925 \text{ mm}^3$ . As  $\alpha_i$  increases to 0.50, the ink volumes on the surfaces of the rollers are almost aligned. Thus, the smallest ink amount is on roller 6, and the largest is on roller 13. However, the ratio between the largest and smallest volumes is only 1.1 and the total ink amount on the rollers increases 1.6 times. When printing imprints with  $k_z = 1.0$  at  $\alpha_i = 0.56$ , the total ink volume on the surfaces of the rollers decreases by 11 % compared to the results at  $\alpha_i = 0.50$ . This changes the nature of the ink volumes distribution: the largest ink amount accumulates on roller 7, and the smallest is on roller 11. It is observed the almost diametrically opposite nature of the ink volume change due to the influence of  $\alpha_i$  at the output of the IPS, i.e. on the surfaces of the PC and BC (Figure 9), compared to the input of system (Figure 7). Thus, the ink volumes on the surfaces PC and BC at  $\alpha_i = 0.40$  are  $V_{PC} = 375 \text{ mm}^3$  and  $V_{BC} = 171 \text{ mm}^3$ , respectively. As  $\alpha_i$  increases to 0.50, the ink volumes increase 2.3 and 3 times, and with  $\alpha_i = 0.56$ , they increase 2.5 and 3.5 times, respectively.

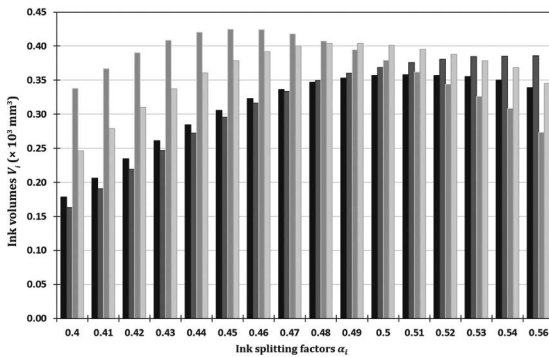


Figure 8: Dependence of the ink volumes on the surfaces of form rollers  $R_6$ ,  $R_7$ ,  $R_{11}$ , and  $R_{13}$  on the factor  $\alpha_i$  when obtaining imprints with  $k_z = 1.0$

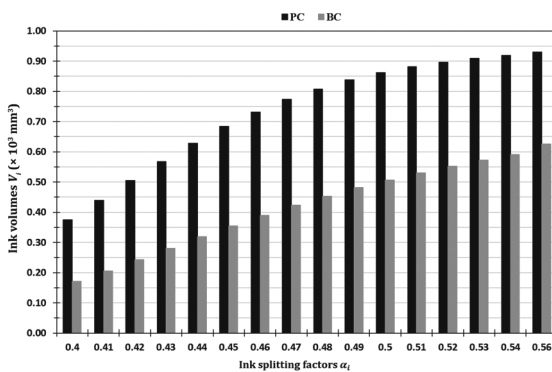


Figure 9: Dependence of the ink volumes on the surfaces of the PC and BC on the factor  $\alpha_i$  when obtaining imprints with  $k_z = 1.0$

The ink amount that accumulates in the IPS after the printing process consists of the sum of the ink volumes in the system without FR ( $V_{IPS^*}$ ) and on the surface of the FR ( $V_{FR}$ ). Its distribution is shown in the diagram in Figure 10. The largest ink amount on the surface of the FR accumulates during the printing imprints with  $k_z = 1.0$  at  $\alpha_i = 0.40$  and is  $V_{FR} = 11880 \text{ mm}^3$ . As  $\alpha_i$  increases, the ink volume on the surface of the FR decreases proportionally, but not significantly. So, at  $\alpha_i = 0.56$  it is  $11200 \text{ mm}^3$ , i.e. decrease by only 6 %. However, the change of  $\alpha_i$  has a completely different effect on the ink amount that accumulates on the surface of all other elements of the IPS  $V_{IPS^*}$ . When printing imprints with  $k_z = 1.0$  at  $\alpha_i = 0.40$ , the ink volume in the IPS is  $V_{IPS^*} = 8243 \text{ mm}^3$ , and the largest volume is obtained at  $\alpha_i = 0.44$ , namely  $V_{IPS^*} = 9478 \text{ mm}^3$ . That is, it is higher than in the previous case, by 15 %. And when receiving imprints at  $\alpha_i = 0.56$ , the ink volume that accumulates,  $V_{IPS^*}$ , is  $6916 \text{ mm}^3$ , and it is 16 % less than that obtained at  $\alpha_i = 0.40$ .

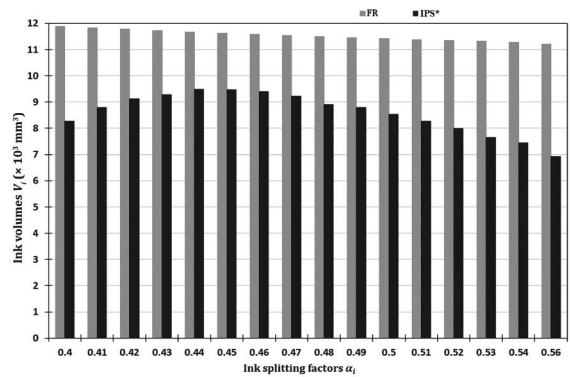


Figure 10: Dependence of ink volumes on the FR and in the IPS without it (IPS\*) on  $\alpha_i$  when obtaining imprints with  $k_z = 1.0$

It is important, both scientifically and practically, to determine whether the same effect of the change  $\alpha_i$  on the distribution of ink volumes on the surfaces of the IPS elements takes place during the production of imprints with a lower density of filling their elements. To perform this task, we reconfigured the simulator subsystem, which generates printing elements, so that the form is reproduced with the same zonal filling coefficients of printing elements in all zones, which are  $k_z = 0.2$ . The value of the total ink supply  $b_d$  is reduced to 10 mm. We set the thickness of the zonal ink supply  $h_d^j$  and conducted a series of model experiments changing the values of the factors  $\alpha_i$  in the range from 0.40 to 0.56.

The results obtained are summarized in Table A.3, and Table A.4 (Appendix A). According to Table A.3 it was constructed a diagram of the ink thickness in the  $j$ -th zones of the imprints with  $k_z = 0.2$  for different values of  $\alpha_i$  (Figure 11).

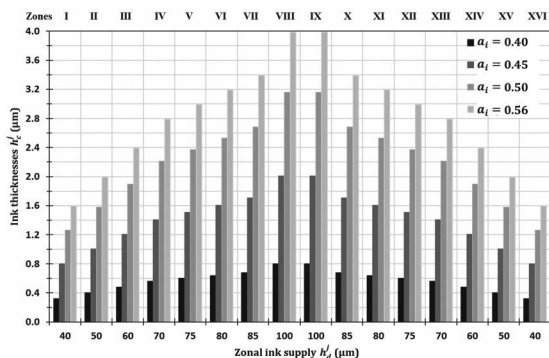


Figure 11: Ink thicknesses in the  $j$ -th zones of imprints with  $k_z = 0.2$  for different factors  $\alpha_i$

As can be seen from the diagram, the nature of the ink thicknesses zonal distribution on the surface of the imprint is similar to that obtained during the replication of imprints with  $k_z = 1.0$ . But in this case, there is a much greater influence of the factors  $\alpha_i$  on the ink thickness of imprints. Thus, with increasing  $\alpha_i$  from 0.40 to 0.45, the ink thickness in all zones of the imprints with  $k_z = 0.2$  increases 2.5 times. And, the thicknesses increase 4 and 5 times with the increase of the splitting factor  $\alpha_i$  to 0.50 and 0.56, respectively. This increase, respectively, is 20 %, 30 % and 40 % greater than when obtaining imprints with  $k_z = 1.0$  (see Figure 5).

According to Table A.4 (Appendix A), the diagrams of ink flows volumes distribution are constructed, presented in Appendix B and in Figure 12.

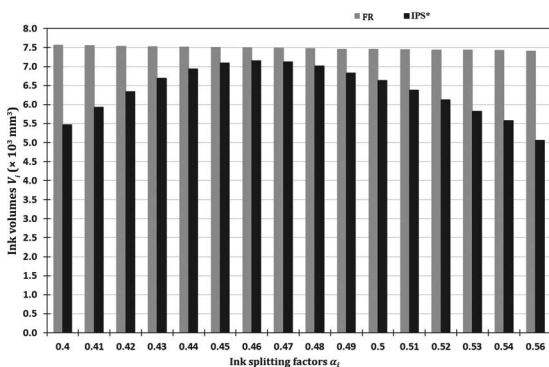


Figure 12: Dependence of ink volumes on the FR and in the IPS (IPS\*) on  $\alpha_i$  when obtaining imprints with  $k_z = 0.2$

From the comparative analysis of the diagrams shown in Figure 6 and Figure B.1 (Appendix B), we can conclude that the IPS is more sensitive to changes in the ink splitting factors when printing imprints with  $k_z = 0.2$ . Thus, in the process of printing imprints with  $k_z = 0.2$  at  $\alpha_i = 0.40$ , the ink volume on the surface of the roller 1 (OR 1) (Figure B.2) is  $V_1 = 1\,388\text{ mm}^3$ . With

an increase of  $\alpha_i$  to 0.56, it decreases by 78 % and this decrease is 10 % greater than when obtaining imprints with  $k_z = 1.0$  (Figure 7). It should be noted that in the process of printing imprints with  $k_z = 1.0$  and  $k_z = 0.2$  according to the diagrams shown in Figure 8 and Figure B.3 (Appendix B), the nature of the ink volumes distributions on the surfaces of the form rollers 6, 7, 11, 13 at the change of  $\alpha_i$  in the range from 0.40 to 0.47 is identical. However, as the ink splitting factors increase, these ink flow volumes distributions on the surfaces of the form rollers are different. Thus, when modeling the process of printing imprints with  $k_z = 1.0$  at  $\alpha_i = 0.56$ , the largest ink amount accumulates on the form roller 7, and when obtaining prints with  $k_z = 0.2$ , it is on the form roller 6.

Comparing the diagrams shown in Figure 8 and Figure B.4 (Appendix B), we can conclude that with increasing values of the factors  $\alpha_i$  there is a more pronounced tendency to accumulate ink on the surfaces of the PC and BC during the printing of imprints with  $k_z = 0.2$ . It should be noted that in the process of obtaining imprints with  $k_z = 1.0$  in the range of change  $\alpha_i$  from 0.40 to 0.56, as shown in Figure 10, the FR accumulates a larger ink volume than the total volume on the surfaces of all other elements of the IPS (IPS\*). However, another trend is observed when simulating the process of printing imprints with  $k_z = 0.2$ . Thus, with a change of  $\alpha_i$  in the range from 0.45 to 0.47, the total ink volume on the surface of all components (IPS\*) does not significantly exceed the ink volume that accumulates on the surface of the FR (Figure 12).

We built a diagram for analyzing the effect of the ink splitting factors  $\alpha_i$  on the IPS ink filling according to Table A.2 and Table A.4 (Appendix A), which is shown in Figure 13.

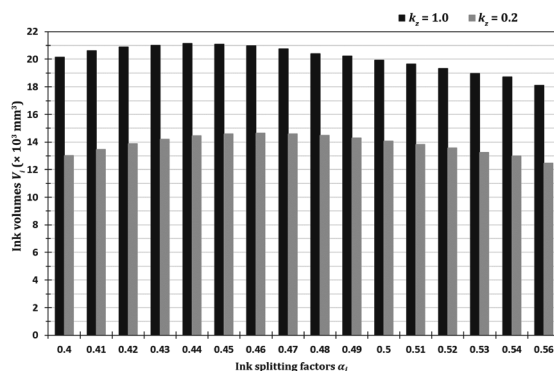


Figure 13: Ink volumes in the GTO-52 offset printing machine system obtained during modeling of the printing process

As can be seen from the diagram, the change of the factors  $\alpha_i$  in a sufficiently wide range does not significantly affect the ink amount accumulated in IPS. A more significant influence on the ink accumulation in

the system has the coverage of the form with printing elements. When replicating imprints with  $k_z = 1.0$ , the largest ink volume in the IPS accumulates at  $\alpha_i = 0.44$  and is  $21148 \text{ mm}^3$ , and the smallest is at  $\alpha_i = 0.56$ , being  $18116 \text{ mm}^3$ . That is, the ink volume that accumulates in the system under the influence of the coefficients  $\alpha_i$  varies from minimum to maximum value by only 16.7 %. A similar trend is characteristic when obtaining imprints with  $k_z = 0.2$ . However, the largest ink volume accumulates in IPS at  $\alpha_i = 0.46$  ( $14645 \text{ mm}^3$ ), and the smallest, as in the previous case, when  $\alpha_i = 0.56$ , when is  $12472 \text{ mm}^3$ . In this case, the ink amount that accumulates in the system under the influence of  $\alpha_i$  varies in the same range as during the replication of imprints with  $k_z = 1.0$ . Although the ink volume increases with decreasing  $\alpha_i$ , the ink thickness on the surface of the imprints with  $k_z = 1.0$  and  $k_z = 0.2$  decreases by 1.96 and 1.76 times, respectively. As a result of the data analysis given in Table A.1, it is established that during the simulation of the process of imprints printing with the maximum coverage of the form surface by image elements ( $k_z = 1.0$ ) at the change of ink splitting factors  $\alpha_i$  from 0.50 to 0.56 ink thickness on the surface of the imprints increases by 23 %. And when receiving imprints at  $\alpha_i = 0.40$ , the ink thickness on the imprints decreases by 66 %. Based on the data obtained by simulating the process of printing imprints with  $k_z = 0.2$  (Table A.2), it was found that when  $\alpha_i$  changes from 0.50 to 0.56, the ink thickness on the surface of the imprints increases by 26 %, and with decreasing  $\alpha_i$  to 0.40 the ink thickness on the imprints is reduced by 75 %. At the same time, the effect of changing the density of form filling with printing elements is not so significant. Thus, at  $\alpha_i = 0.40$ , the ink thickness on the imprints with  $k_z = 0.2$  is less by 12 % compared to the ink thickness on the surface of the imprints with  $k_z = 1.0$ . And at  $\alpha_i = 0.56$ , this thickness becomes greater by only 3 % relative to the ink thickness on the imprint with  $k_z = 1.0$ . Therefore, the efficiency of the automatic adjusting system is significantly reduced when determining the parameters

of the previous adjusting, provided that the value of the coefficients  $\alpha_i$  in all zones of the IPS elements is 0.50, but in reality, it will be different. In this case, it will be needed to adjust the parameters of the input task already in the printing process.

#### 4. Conclusions

The research of the ink transfer process, which takes place in the IPS of the offset machine during printing, was carried out with the help of the developed method utilising computer technology. The influence of the ink splitting factors change in the contact zones of rollers and cylinders on the redistribution of ink flows in the IPS is established. As the ink splitting factors decrease from 0.50, the ink volumes on the surfaces of the rollers and cylinders close to the system input increase. As the splitting factors increase, there is a tendency to increase the ink volume on the surfaces of the elements close to the system output. However, both at the minimum and at the maximum value of the splitting factors  $\alpha_i$ , the total ink volume in the IPS is not the maximum. The maximum is achieved in the duplication process of imprints from the printing plate with  $k_z = 0.2$  at the ink splitting factors  $\alpha_i = 0.46$ . And the maximum ink volume when printing imprints with  $k_z = 1.0$  is obtained at the ink splitting factor of 0.44. The ink thickness on the surface of the imprints significantly depends on the change of ink splitting factors in the contact zones of the rollers and cylinders. Therefore, the value of the ink splitting factors must be taken into account at the stage of the previous adjusting of the IPS. The proposed method makes it possible to determine the ink consumption for printing jobs, taking into account the ink amount that accumulates in the IPS during printing. To obtain reliable information about the value of ink splitting during printing, it is necessary to develop an appropriate methodology, the testing of which requires thorough experimental research.

#### References

- Chu, H., Lin, X. and Cai, L., 2019. Analysis of temperature characteristics of ink fluid based on power law model in microchannel. *Advances in Mechanical Engineering*, 11(3), pp. 1–15. <https://doi.org/10.1177/1687814019833585>.
- Claypole, J., Williams, P.R. and Deganello, D., 2012. Control of breakup of ink filaments in offset printing. In: N. Enlund and M. Lovreček, eds. *Advances in Printing and Media Technology: Proceedings of the 39<sup>th</sup> International Research Conference of Iarigai*. Ljubljana, Slovenia, September 2012, pp. 207–211.
- Kapović, D., Rožić, M., Vukoje, M. and Lozo, B., 2019. Ink tack stability readings of the offset thermochromic inks. *Pigment & Resin Technology*, 48(4), pp. 309–316. <https://doi.org/10.1108/PRT-07-2018-0064>.
- Kipphan, H. ed., 2001. *Handbook of print media*. Berlin, New York: Springer.
- Liu, L., Li, K. and Lu, F., 2016. Dynamic simulation modeling of inking system based on elastohydrodynamic lubrication. *International Journal of Heat and Technology*, 34(1), pp. 124–128. <https://doi.org/10.18280/ijht.340118>.
- Ma, J.-J., 2010. Relationship between temperature and ink transferring of the inking system and its control. *Journal of University of Shanghai for Science and Technology*, 6, pp. 609–612.
- MacPhee, J., 1998. *Fundamentals of lithographic printing*. Pittsburgh, PA, USA: GATF Press.

- MathWorks, 2020. *Simulink is for model-based design*. [online] Available at: <<https://www.mathworks.com/products/simulink.html>> [Accessed 5 July 2020].
- Rech, H., 1971. *Beiträge zur experimentellen und rechnerischen Untersuchung des Farbtransportes in Walzenfarbwerken von Druckmaschinen*. Dr.-Ing. Dissertation. Technische Hochschule Darmstadt. <https://tuprints.ulb.tu-darmstadt.de/id/eprint/13556>.
- Romano, R., 2015. Offset lithography: the future ain't what it used to be. *Nitto printing*, [blog] 14 April. Available at: <[http://www.nittoprinting.com/v1/news.php?news\\_id=15&start=4&category](http://www.nittoprinting.com/v1/news.php?news_id=15&start=4&category)> [Accessed December 2021].
- Shen, Y.-H., Cheng, H.-C., Chen, Y.-W., Lu, S.-T., Lin, S.-M. and Chen, W.-H., 2017. Temperature effects on ink transfer performance of gravure offset printing for fine-line circuitry. In: *IEEE 2017 International Conference on Electronics Packaging (ICEP)*. Yamagata, Japan, 19–22 April 2017. IEEE, pp. 475–478. <https://doi.org/10.23919/ICEP2017.7939424>.
- Tyagi, A.K., 2012. *MATLAB and Simulink for engineers*. New Delhi, India: Oxford University Press.
- Verkhola, M.I. and Huk, I.B., 2009. Modeliuvannia ta vyznachennia koefitsiienta peredachi farby peredavalnym valykom u farbovii systemi z roztyrnyym tsylindrom. *Komp'uterni tekhnologii drukarstva*, 21, pp. 39–52. (In English: Modeling and determination of ink transfer coefficient by transfer roller at ink system with grinding cylinder. *Computer Technologies of Printing*).
- Verkhola, M., Huk, I., Panovyk, U. and Spolyak, R., 2015. Information technology of verification of models authenticity of ink printing systems with the drum cylinders. *Technological Complexes*, 11(1/1), pp. 53–63.
- Verkhola, M., Panovyk, U., Huk, I. and Kalytka, M., 2019. Modeling of the ink printing system and improving the accuracy of its adjustment based on the obtained three-dimensional imprints. In: N. Kryvinska, I. Izonin, M. Greguš, A. Poniszewska-Marañda and I. Dronyuk, eds. *Proceedings of the 1st International Workshop on Digital Content & Smart Multimedia (DCSMart)*. Lviv, Ukraine, 23–25 December 2019, pp. 292–302. (pdf) Available at: <<http://ceur-ws.org/Vol-2533/paper27.pdf>> [Accessed December 2021].
- Verkhola, M.I. and Kalytka, M.I., 2019. Modelyuvannia ta analiz vplyvu tekhnolohichnykh parametriv na rozpodil ob'yemiv potokiv farby u farbodrukars'kyi systemi poslidojno-paralel'noyi struktury. *Modelyuvannia ta informatsiyni tekhnolohiyi*, 88, pp. 225–242. (In English: Modeling and analysis of technological parameters influence on the ink flow volume's distribution in the ink printing system of serial-parallel structure, *Modeling and Information Technologies*). <http://doi.org/10.5281/zenodo.3862078>.
- Vlachopoulos, G., Claypole, T. and Bould, D., 2010. Ink mist formation in roller trains. In: N. Enlund and M. Lovreček, eds. *Advances in Printing and Media Technology: Proceedings of the 37<sup>th</sup> International Research Conference of IARIGAI*. Montreal, Canada, September 2010, pp. 227–234.

**Appendix A: Data of model experiments**

*Table A.1: Ink thicknesses  $h_c^j$  ( $\mu\text{m}$ ) in the  $j$ -th zones of the offset machine GTO-52, for imprints with  $k_z = 1.0$*

Zonal	Ink splitting factor $\alpha_i$															
ink supply	0.40	0.41	0.42	0.43	0.44	0.45	0.46	0.47	0.48	0.49	0.50	0.51	0.52	0.53	0.54	0.56
$h_d$ ( $\mu\text{m}$ )	Ink thickness $h_c^j$ ( $\mu\text{m}$ )															
65	0.416	0.501	0.591	0.683	0.775	0.865	0.950	1.030	1.104	1.171	1.233	1.291	1.343	1.392	1.437	1.521
70	0.448	0.539	0.636	0.736	0.835	0.931	1.023	1.109	1.189	1.261	1.328	1.390	1.447	1.499	1.548	1.638
90	0.576	0.693	0.818	0.946	1.074	1.197	1.315	1.426	1.529	1.622	1.708	1.787	1.860	1.927	1.990	2.105
100	0.640	0.770	0.909	1.051	1.193	1.330	1.461	1.584	1.699	1.802	1.897	1.985	2.066	2.141	2.211	2.339
120	0.768	0.925	1.091	1.262	1.431	1.596	1.754	1.901	2.038	2.162	2.277	2.383	2.480	2.569	2.654	2.807
130	0.832	1.002	1.182	1.367	1.551	1.730	1.900	2.059	2.208	2.342	2.467	2.581	2.686	2.783	2.875	3.041
140	0.896	1.079	1.273	1.472	1.670	1.863	2.046	2.218	2.378	2.523	2.656	2.780	2.893	2.998	3.096	3.275
150	0.960	1.156	1.364	1.577	1.789	1.996	2.192	2.376	2.548	2.703	2.846	2.978	3.100	3.212	3.317	3.509
150	0.960	1.156	1.364	1.577	1.789	1.996	2.192	2.376	2.548	2.703	2.846	2.978	3.100	3.212	3.317	3.509
140	0.896	1.079	1.273	1.472	1.670	1.863	2.046	2.218	2.378	2.523	2.656	2.780	2.893	2.998	3.096	3.275
130	0.832	1.002	1.182	1.367	1.551	1.730	1.900	2.059	2.208	2.342	2.467	2.581	2.686	2.783	2.875	3.041
120	0.768	0.925	1.091	1.262	1.431	1.596	1.754	1.901	2.038	2.162	2.277	2.383	2.480	2.569	2.654	2.807
100	0.640	0.770	0.909	1.051	1.193	1.330	1.461	1.584	1.699	1.802	1.897	1.985	2.066	2.141	2.211	2.339
85	0.544	0.655	0.773	0.894	1.014	1.131	1.242	1.346	1.444	1.532	1.613	1.688	1.757	1.820	1.880	1.988
65	0.416	0.501	0.591	0.683	0.775	0.865	0.950	1.030	1.104	1.171	1.233	1.291	1.343	1.392	1.437	1.521
60	0.384	0.462	0.545	0.631	0.716	0.798	0.877	0.950	1.019	1.081	1.138	1.191	1.240	1.285	1.327	1.404

*Table A.2: Distribution of ink volumes  $V_i$  ( $\times 10^3 \text{ mm}^3$ ) in the IPS of the offset machine GTO-52, for imprints with  $k_z = 1.0$*

Elements	Ink splitting factor $\alpha_i$															
IPS	0.40	0.41	0.42	0.43	0.44	0.45	0.46	0.47	0.48	0.49	0.50	0.51	0.52	0.53	0.54	0.56
	Ink volumes $V_i$ ( $\times 10^3 \text{ mm}^3$ )															
VR	0.509	0.490	0.468	0.442	0.416	0.389	0.363	0.338	0.316	0.296	0.279	0.264	0.251	0.240	0.230	0.215
1	2.143	2.149	2.104	1.956	1.906	1.749	1.622	1.464	1.282	1.242	1.118	1.042	0.958	0.853	0.814	0.693
2	1.200	1.267	1.249	1.206	1.186	1.138	1.078	1.015	1.903	0.875	0.818	0.755	0.702	0.636	0.609	0.528
3	0.898	0.961	0.980	0.988	0.987	0.971	0.943	0.907	0.843	0.818	0.771	0.723	0.678	0.629	0.595	0.520
4	0.441	0.477	0.508	0.532	0.546	0.553	0.552	0.545	0.529	0.514	0.496	0.473	0.451	0.426	0.407	0.362
5	0.342	0.383	0.422	0.457	0.484	0.504	0.518	0.524	0.528	0.522	0.514	0.503	0.489	0.474	0.457	0.423
6	0.380	0.409	0.434	0.452	0.461	0.463	0.458	0.447	0.434	0.414	0.393	0.371	0.348	0.325	0.302	0.259
7	0.263	0.269	0.299	0.327	0.350	0.368	0.383	0.392	0.398	0.399	0.398	0.394	0.388	0.380	0.371	0.351
8	0.228	0.259	0.288	0.314	0.336	0.354	0.366	0.374	0.378	0.378	0.375	0.369	0.361	0.352	0.341	0.318
9	0.396	0.437	0.472	0.500	0.519	0.530	0.534	0.530	0.520	0.505	0.487	0.466	0.443	0.420	0.396	0.350
10	0.178	0.206	0.234	0.261	0.285	0.306	0.323	0.336	0.347	0.353	0.357	0.358	0.357	0.355	0.350	0.339
11	0.163	0.191	0.219	0.247	0.272	0.296	0.316	0.334	0.350	0.360	0.360	0.376	0.381	0.385	0.385	0.386
12	0.338	0.367	0.390	0.409	0.420	0.425	0.424	0.418	0.408	0.394	0.379	0.362	0.344	0.326	0.308	0.274
13	0.246	0.279	0.310	0.337	0.361	0.379	0.392	0.400	0.404	0.404	0.401	0.396	0.388	0.379	0.368	0.345
PC	0.375	0.440	0.505	0.568	0.628	0.684	0.731	0.773	0.807	0.838	0.862	0.881	0.897	0.908	0.918	0.930
BC	0.171	0.206	0.243	0.280	0.318	0.355	0.390	0.423	0.453	0.481	0.507	0.530	0.552	0.572	0.591	0.626
IPS*	8.271	8.790	9.125	9.276	9.475	9.464	9.393	9.220	8.900	8.793	8.520	8.270	7.990	7.650	7.440	6.919
FR	11.88	11.83	11.78	11.72	11.67	11.62	11.58	11.53	11.49	11.45	11.42	11.38	11.34	11.31	11.27	11.20
IPS	20.15	20.62	20.91	20.99	21.15	21.08	20.97	20.75	20.39	20.24	19.94	19.65	19.33	18.96	18.71	18.12

Table A.3: Ink thicknesses  $h_c^j$  ( $\mu\text{m}$ ) in the  $j$ -th zones of the offset machine GTO-52, for imprints with  $k_z = 0.2$

Zonal ink supply $h_d$ ( $\mu\text{m}$ )	Ink splitting factor $\alpha_i$															
	0.40	0.41	0.42	0.43	0.44	0.45	0.46	0.47	0.48	0.49	0.50	0.51	0.52	0.53	0.54	0.56
	Ink thickness $h_c^j$ ( $\mu\text{m}$ )															
40	0.320	0.401	0.493	0.592	0.697	0.803	0.907	1.007	1.101	1.186	1.263	1.334	1.397	1.453	1.505	1.595
50	0.400	0.501	0.616	0.740	0.871	1.004	1.134	1.259	1.376	1.482	1.579	1.667	1.746	1.816	1.881	1.994
60	0.480	0.602	0.739	0.888	1.045	1.204	1.361	1.511	1.351	1.779	1.895	2.001	2.095	2.179	2.257	2.393
70	0.560	0.702	0.862	1.036	1.220	1.405	1.588	1.763	1.927	2.075	2.211	2.334	2.444	2.543	2.633	2.792
75	0.600	0.752	0.924	1.110	1.307	1.506	1.701	1.889	2.064	2.224	2.369	2.501	2.619	2.724	2.821	2.991
80	0.640	0.802	0.985	1.184	1.394	1.606	1.815	2.015	2.202	2.372	2.527	2.667	2.793	2.906	3.009	3.190
85	0.680	0.852	1.047	1.258	1.481	1.706	1.928	2.141	2.339	2.520	2.685	2.834	2.968	3.087	3.197	3.390
100	0.799	1.003	1.232	1.480	1.742	2.007	2.268	2.519	2.752	2.965	3.159	3.334	3.492	3.632	3.761	3.988
100	0.799	1.003	1.232	1.480	1.742	2.007	2.268	2.519	2.752	2.965	3.159	3.334	3.492	3.632	3.761	3.988
85	0.640	0.852	1.047	1.258	1.481	1.706	1.928	2.141	2.339	2.520	2.685	2.834	2.968	3.087	3.197	3.390
80	0.640	0.802	0.985	1.184	1.394	1.606	1.815	2.015	2.202	2.372	2.527	2.667	2.793	2.906	3.009	3.190
75	0.600	0.752	0.924	1.110	1.307	1.506	1.701	1.889	2.064	2.224	2.369	2.501	2.619	2.724	2.821	2.991
70	0.560	0.702	0.862	1.036	1.220	1.405	1.588	1.763	1.927	2.075	2.211	2.334	2.444	2.543	2.633	2.792
60	0.480	0.602	0.739	0.888	1.045	1.204	1.361	1.511	1.651	1.779	1.895	2.001	2.095	2.179	2.257	2.393
50	0.400	0.501	0.616	0.740	0.871	1.004	1.134	1.259	1.376	1.482	1.579	1.667	1.746	1.816	1.881	1.994
40	0.320	0.401	0.493	0.592	0.697	0.803	0.907	1.007	1.101	1.186	1.263	1.334	1.397	1.453	1.505	1.595

Table A.4: Distribution of ink volumes  $V_i$  ( $\times 10^3 \text{ mm}^3$ ) in the IPS of the offset machine GTO-52, for imprints with  $k_z = 0.2$

Elements	Ink splitting factor $\alpha_i$															
IPS	0.40	0.41	0.42	0.43	0.44	0.45	0.46	0.47	0.48	0.49	0.50	0.51	0.52	0.53	0.54	0.56
	Ink volumes $V_i$ ( $\times 10^3 \text{ mm}^3$ )															
VR	0.299	0.289	0.275	0.258	0.238	0.217	0.195	0.173	0.153	0.135	0.119	0.105	0.093	0.083	0.074	0.062
1	1.388	1.386	1.361	1.311	1.250	1.176	1.073	0.971	0.865	0.742	0.668	0.587	0.523	0.432	0.391	0.304
2	0.796	0.832	0.842	0.845	0.836	0.800	0.764	0.712	0.658	0.605	0.542	0.488	0.435	0.380	0.344	0.274
3	0.593	0.644	0.692	0.722	0.730	0.731	0.721	0.699	0.668	0.636	0.587	0.543	0.499	0.499	0.417	0.344
4	0.298	0.336	0.371	0.403	0.428	0.446	0.456	0.458	0.454	0.443	0.428	0.410	0.389	0.367	0.345	0.302
5	0.255	0.299	0.343	0.387	0.427	0.462	0.490	0.512	0.526	0.532	0.534	0.530	0.522	0.511	0.497	0.465
6	0.138	0.168	0.201	0.236	0.270	0.304	0.335	0.362	0.386	0.406	0.422	0.435	0.444	0.451	0.456	0.459
7	0.127	0.156	0.187	0.219	0.252	0.284	0.314	0.342	0.366	0.386	0.403	0.417	0.428	0.437	0.443	0.450
8	0.289	0.325	0.359	0.388	0.412	0.428	0.437	0.439	0.433	0.422	0.407	0.389	0.369	0.347	0.325	0.281
9	0.190	0.224	0.259	0.294	0.327	0.357	0.381	0.400	0.414	0.422	0.426	0.426	0.423	0.417	0.409	0.382
10	0.187	0.221	0.255	0.289	0.321	0.348	0.371	0.387	0.398	0.403	0.403	0.399	0.392	0.382	0.370	0.341
11	0.298	0.336	0.370	0.400	0.423	0.440	0.448	0.449	0.443	0.431	0.415	0.396	0.376	0.354	0.331	0.287
12	0.330	0.378	0.425	0.467	0.503	0.530	0.547	0.555	0.554	0.544	0.529	0.508	0.484	0.458	0.431	0.375
13	0.193	0.230	0.268	0.305	0.340	0.371	0.396	0.416	0.430	0.437	0.440	0.438	0.432	0.423	0.412	0.385
PC	0.061	0.075	0.089	0.104	0.120	0.134	0.148	0.160	0.171	0.180	0.187	0.193	0.198	0.201	0.204	0.207
BC	0.028	0.035	0.043	0.052	0.061	0.070	0.079	0.088	0.096	0.103	0.110	0.116	0.122	0.127	0.131	0.139
IPS*	5.469	5.931	6.341	6.688	6.941	7.096	7.154	7.122	7.014	6.828	6.630	6.380	6.128	5.818	5.580	5.062
FR	7.559	7.549	7.537	7.526	7.513	7.502	7.491	7.481	7.472	7.453	7.455	7.447	7.439	7.432	7.424	7.410
IPS	13.03	13.48	13.88	14.21	14.45	14.60	14.65	14.60	14.49	14.28	14.09	13.83	13.57	13.25	13.00	12.47

**Appendix B: Graphical representation of model experiments**

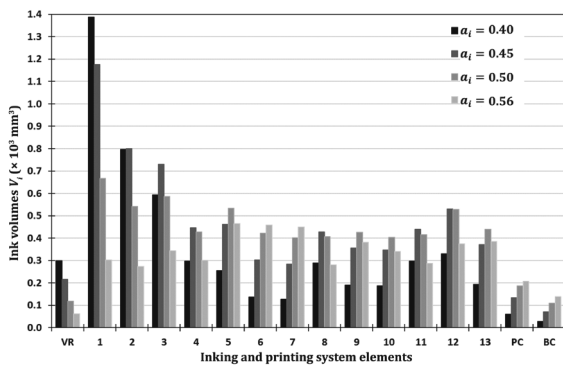


Figure B.1: Distributions of ink flow volumes in the IPS with  $k_z = 0.2$  for different values of  $\alpha_i$

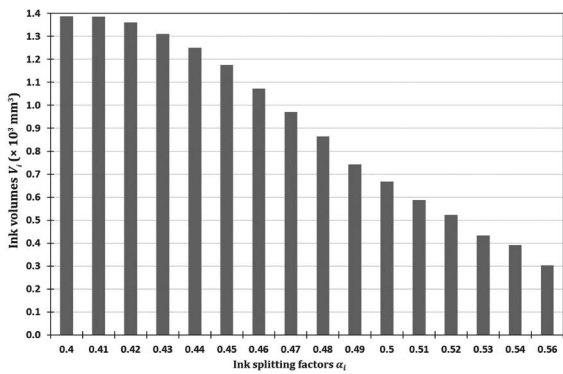


Figure B.2: Dependence of the ink volume at the surface of the roller 1 on the splitting coefficients  $\alpha_i$  with  $k_z = 0.2$

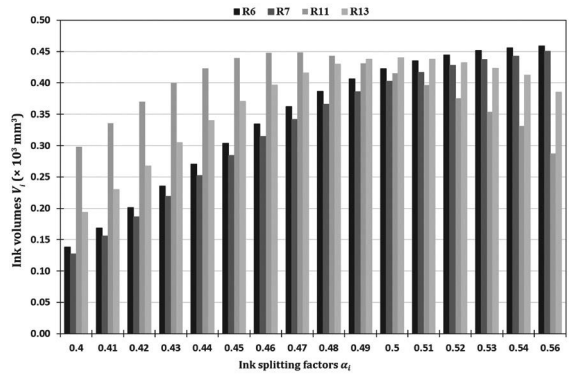


Figure B.3: Dependence of the ink volumes at the surfaces of the form rollers  $R_6$ ,  $R_7$ ,  $R_{11}$ , and  $R_{13}$  on the splitting coefficients  $\alpha_i$  with  $k_z = 0.2$

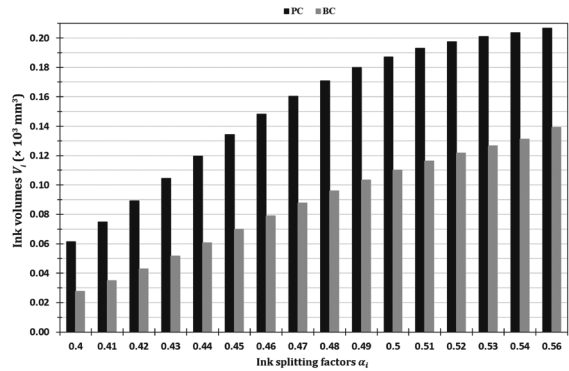


Figure B.4: Dependence of the ink volumes on the surfaces of the PC and BC on the factors  $\alpha_i$  with  $k_z = 0.2$

